

Control of chemo-hydrodynamic pattern formation by external localized cooling

D. A. BRATSUN¹, Y. SHI², K. ECKERT² and A. DE WIT¹

¹ *Service de Chimie Physique and Center for Nonlinear Phenomena and Complex Systems, CP 231, Université Libre de Bruxelles - 1050 Brussels, Belgium*

² *Institute for Aerospace Engineering, Dresden University of Technology 01062 Dresden, Germany*

received 27 September 2004; accepted in final form 3 January 2005

published online 2 February 2005

PACS. 47.70.Fw – Chemically reactive flows.

PACS. 47.70.-n – Reactive, radiative, or nonequilibrium flows.

PACS. 47.20.Bp – Buoyancy-driven instability.

Abstract. – Chemo-hydrodynamic patterns can form in a chemical two-layer system in a Hele-Shaw cell when each fluid contains separately a reactant of an exothermic neutralization reaction. When one reactant diffuses through the interface, the coupling between the chemical reaction and buoyancy-driven flows gives rise to complex spatio-temporal fingering near the interface. We show both experimentally and theoretically that such chemistry-driven fingering and its characteristics can be precisely controlled by external cooling applied locally along the sidewalls of the reactor. This control process gives a bright example of cooperative phenomena between chemistry and hydrodynamics and offers promising technological applications.

The study of pattern formation in reactive two-layer systems of immiscible fluids is interesting both from a fundamental point of view and with respect to potential applications ranging from petroleum and nuclear to pharmaceutical engineering as well as food production. The spontaneous generation of convective flows at the interface is of practical importance because it leads to mechanisms of mass transfer which are much more efficient than molecular diffusion and can drastically alter pattern formation in the system. One such mechanism is a hydrodynamic instability of Rayleigh-Taylor type which occurs when denser chemicals lie in a Hele-Shaw cell (two glass plates separated by a thin gap width) on top of lighter ones in the gravitational field. This situation and other chemo-hydrodynamic instabilities at interfaces have received increasing attention these last years both from experimental [1–7] and theoretical [8–11] points of view.

On the other hand, the control of pattern formation in spatially distributed systems is an important goal for applications where a specific spatio-temporal dynamics or the suppression of the instability is desired. In that respect, temporal [12] or spatio-temporal [13] periodic forcing of spatially extended oscillatory chemical systems can lead, among others, to entrainment of spiral tip trajectories [14], formation of labyrinthine patterns [15] or even complex patterns characterized by multiple length scales [13]. In the same spirit, reaction-diffusion patterns such

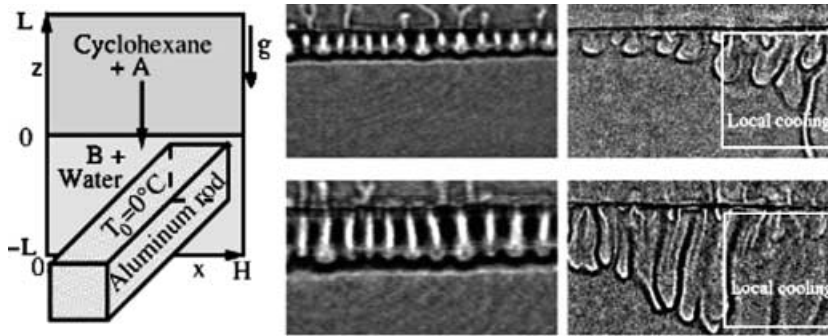


Fig. 1 – Sketch of the system (not drawn to scale; only one cooling rod is shown for clarity) and experimental visualization of the influence of local cooling on pattern formation in a Hele-Shaw cell of gap width 0.5 mm. The initial concentration of acid A and base B are both 0.25 mol/l. The second and third columns focus on the lower part of the system (the black horizontal line corresponding to the location of the interface at $z = 0$) and show the chemo-hydrodynamic pattern, respectively, without and with localized cooling at successive dimensional times $t = 20$ min and 40 min.

as Turing structures, for instance, can be controlled, *i.e.* their stability domain, symmetry or wavelength can be modified, by application of electric fields [16] or modulated light [17, 18]. The control of hydrodynamic patterns has also been achieved by manipulating the flows thermally [19, 20], optically [21] or by application of sinusoidal vibrations [22], to name a few. The control of pattern formation in systems where chemical reactions, diffusion and convection are simultaneously operative remains however largely unstudied.

In this letter, we show both experimentally and theoretically that mixed reaction-diffusion-convection systems can be controlled by using a localized cooling applied externally along the wall of the reactor. As a consequence, the chemo-hydrodynamic pattern and its characteristics can be externally changed in order to enhance or slow down at wish the yield of the reaction and the mass transfer across the interface.

Experiments were performed in a Hele-Shaw cell containing two immiscible liquid phases in contact along a planar interface (see fig. 1) located at $z = 0$ with the coordinate axes x , z directed along the horizontal and vertical sides of the cell, respectively [4, 5]. The reacting species are propionic acid dissolved in the upper cyclohexane layer and tetramethylammoniumhydroxide (TMAH) dissolved in the lower aqueous layer. These species are involved in a neutralization reaction of propionic acid by TMAH to form a salt (TMA-propionate). This reaction takes place solely in the aqueous phase upon diffusion of acid into the lower layer. The walls of the vertically oriented Hele-Shaw cell are made of a borosilicate float glass with a thickness of 6.50 mm. The sheets of glass are mounted in a rubber-coated aluminium frame and screwed together. For the sealing of the gap between the glass plates, teflon foil allowing for a gap width of (0.50 ± 0.05) mm is used. The cell is filled by means of syringes. The reaction starts after slowly removing a teflon strip initially separating the two liquids. Visualization of the pattern is done by a shadowgraph technique.

The characteristics of pattern formation and the corresponding driving mechanisms have been discussed in detail in [5]. In summary, a regular convective cellular structure forms in the lower layer and slowly penetrates into the bulk. The cells are confined from above by the interface ($z = 0$) and from below by the reaction front (see fig. 1, second column). The formation of the cells is initiated by the coupling between Rayleigh-Taylor instability and chemistry. The interfacial boundary layer formed in the lower layer by acid diffusion in

connection with the chemical reaction is unstable since the acid and salt solutions are heavier than the bulk alkaline solution. Hence the system is prone to a Rayleigh-Taylor instability for vertically oriented cells (*i.e.* where gravity points perpendicularly to the interface). The synchronization of the fingers towards a regular cellular pattern is managed by the double vortex accompanying each finger. The vortices are fed by the permanent conversion of the acid into the lighter salt under release of the reaction enthalpy together with an enhanced acid flux from the upper layer [4,5]. In that way lateral differences in buoyancy are sustained which drive the penetrative convection observed. The chemo-hydrodynamic pattern produced is characterized by a well-defined wavelength which, in the absence of any control, is a function of the nature and concentration of the reactants as well as of the properties of the fluids, the gap width and the heat conductivity of the Hele-Shaw plates.

To check the influence of heat fluxes through the lateral plates of the Hele-Shaw cell, we have locally reduced the outside temperature of one glass plate in an area of 3 cm × 3 cm below the cyclohexane-water interface. This was done by pressing cold aluminum rods against the outside part of the glass plates 5 minutes after reaction onset. The aluminum rods were cooled to 0 °C which is 20 K below the initial temperature of the Hele-Shaw cell. After 5 minutes of local cooling, the aluminum rods were removed. In fig. 1, the second column shows the chemo-hydrodynamic pattern at two successive times evolving at room temperature. The third column shows the controlled system after a local cooling. A significant acceleration of the reaction front is observed inside the cooled area because of enhanced convective motions. Moreover, this faster fluid movement in the cooled area destroys also the regular cellular structure in the non-cooled area. After stopping the cooling, the system slowly recovers and the regular cells form again. This cooling mechanism can be applied to control the chemo-hydrodynamic pattern as we show it now theoretically.

Our model system is, as in experiments, a two-layer system consisting of two immiscible liquid solvents, separated by a plane and undeformable interface, and confined by two vertical parallel solid plates. We assume that an acid A , dissolved in the upper layer, diffuses through the interface to react with a base B , dissolved in the lower layer, to form a salt S with heat release. Such an $A + B \rightarrow S$ neutralization reaction characterized by a reaction rate constant K takes place solely in the lower phase. The gap width $2d$ between the plates is assumed to be much smaller than their lateral extension which leads us to use a Hele-Shaw approximation, *i.e.* 2D gap-averaged Navier-Stokes equations [11]. This procedure reduces the system geometry ($0 < x < H$, $-L < z < L$) to two 2D regions separated by a line $z = 0$. We assume also that surface tension does not play any role in the dynamics and that, without any loss of generality, all chemical species have the same diffusion coefficient D_1 in the lower phase. We choose the following characteristic scales: length $2d$, time $(2d)^2/D_1$, velocity $D_1/2d$, pressure $\rho_1 \nu_1 D_1 / (2d)^2$, concentration A_0 , temperature $QA_0/\rho_1 c_{p1}$, where Q is the reaction enthalpy and c_{p1} is the heat capacity of water at constant pressure. The dimensionless governing equations derived in [11] and written in the Boussinesq approximation are then

$$\nabla \cdot \vec{v}_1 = 0, \quad (1)$$

$$\frac{1}{Sc} \left(\frac{\partial \vec{v}_1}{\partial t} + \frac{6}{5} \vec{v}_1 \cdot \nabla \vec{v}_1 \right) = -\nabla p_1 + \Delta \vec{v}_1 - 12\vec{v}_1 + (LeRT_1 + R_A A_1 + R_B B + R_S S)\vec{z}, \quad (2)$$

$$\frac{\partial T_1}{\partial t} + \frac{3}{5} \frac{(5 + 2Bi)}{(3 + Bi)} \vec{v}_1 \cdot \nabla T_1 = Le\Delta T_1 - \frac{12LeBi}{(3 + Bi)} T_1 + D_a A_1 B, \quad (3)$$

$$\frac{\partial A_1}{\partial t} + \vec{v}_1 \cdot \nabla A_1 = \Delta A_1 - D_a A_1 B, \quad (4)$$

$$\frac{\partial B}{\partial t} + \vec{v}_1 \cdot \nabla B = \Delta B - D_a A_1 B, \quad (5)$$

TABLE I – List of important dimensionless parameters with their estimations based on experimental data.

$Sc = \nu_1/D_1$	Schmidt number	980
$Le = \chi_1/D_1$	Lewis number	131
$D_a = (2d)^2 KA_0/D_1$	Damköhler number	0.1
$R = g\beta_T Q A_0(2d)^3/\kappa_1\nu_1$	thermal Rayleigh number	500
$R_A = g\beta_A A_0(2d)^3/D_1\nu_1$	acid Rayleigh number	-2190
$R_B = g\beta_B A_0(2d)^3/D_1\nu_1$	base Rayleigh number	-1750
$R_S = g\beta_S A_0(2d)^3/D_1\nu_1$	salt Rayleigh number	-1090
$Bi = d\gamma_T/\kappa_1$	Biot number	0 or ∞

$$\frac{\partial S}{\partial t} + \vec{v}_1 \cdot \nabla S = \Delta S + D_a A_1 B, \quad (6)$$

for the lower layer. For the upper layer we get

$$\nabla \cdot \vec{v}_2 = 0, \quad (7)$$

$$\frac{1}{Sc} \left(\frac{\partial \vec{v}_2}{\partial t} + \frac{6}{5} \vec{v}_2 \cdot \nabla \vec{v}_2 \right) = -\frac{1}{\rho} \nabla p_2 + \nu \Delta \vec{v}_2 - 12\nu \vec{v}_2 + (\beta Le RT_2 + \beta_A R_A A_2) \vec{z}, \quad (8)$$

$$\frac{\partial T_2}{\partial t} + \frac{3}{5} \frac{(5 + 2Bi)}{(3 + Bi)} \vec{v}_2 \cdot \nabla T_2 = \chi Le \Delta T_2 - \chi \frac{12Le Bi}{(3 + Bi)} T_2, \quad (9)$$

$$\frac{\partial A_2}{\partial t} + \vec{v}_2 \cdot \nabla A_2 = D \Delta A_2. \quad (10)$$

The boundary conditions are

$$\begin{aligned} z = -L : \vec{v}_1 = 0, \quad \frac{\partial T_1}{\partial z} = 0, \quad \frac{\partial A_1}{\partial z} = 0, \quad \frac{\partial B}{\partial z} = \frac{\partial S}{\partial z} = 0, \\ z = L : \vec{v}_2 = 0, \quad \frac{\partial T_2}{\partial z} = 0, \quad \frac{\partial A_2}{\partial z} = 0, \\ z = 0 : T_1 = T_2, \quad A_1 = k A_2, \quad \vec{v}_1 = \vec{v}_2, \\ \frac{\partial T_1}{\partial z} = \kappa \frac{\partial T_2}{\partial z}, \quad \frac{\partial A_1}{\partial z} = \frac{\partial A_2}{\partial z}, \quad \frac{\partial v_{x1}}{\partial z} = \eta \frac{\partial v_{x2}}{\partial z} \end{aligned} \quad (11)$$

and periodic boundary conditions are applied at the vertical boundaries $x = 0, H$. Here \vec{v}_i and T_i are the gap-averaged velocity and temperature. A_0 is the initial concentration of acid, and the ratios between densities, dynamic and kinematic viscosities, heat conductivities, temperature diffusivities and acid diffusivities as well as the partition ratio, the thermal and solutal expansion coefficients of the upper and lower layers are denoted, respectively, by $\rho, \eta, \nu, \kappa, \chi, D, k, \beta, \beta_A$. Equations (2), (8) differ from Navier-Stokes equations by the additional dissipative terms, which may be interpreted as the average friction force due to the plates. Similarly, heat equations (3), (9) contain terms relating to the process of heat dissipation through the solid plates. The important dimensionless parameters with estimations based on experimental data are listed in table I. Other values are $\eta = 0.96, \nu = 1.1, \kappa = 0.231, \chi = 0.592, k = 1, \beta = 1.0, \beta_A = 1.83, D = 1.0$. The Biot number $Bi = d\gamma_T/\kappa_1$, where γ_T is the heat exchange coefficient between the fluid and the solid walls, is the important parameter related to the intensity of heat losses through the plates. Depending on the plates properties, the Biot number Bi may take a value from 0 (thermo-isolated plates) to ∞ (highly conductive plates). To model the local cooling of sidewalls, we have numerically integrated the above model expressed in the stream function formalism [11] with $Bi = \infty$ in the cooled area and

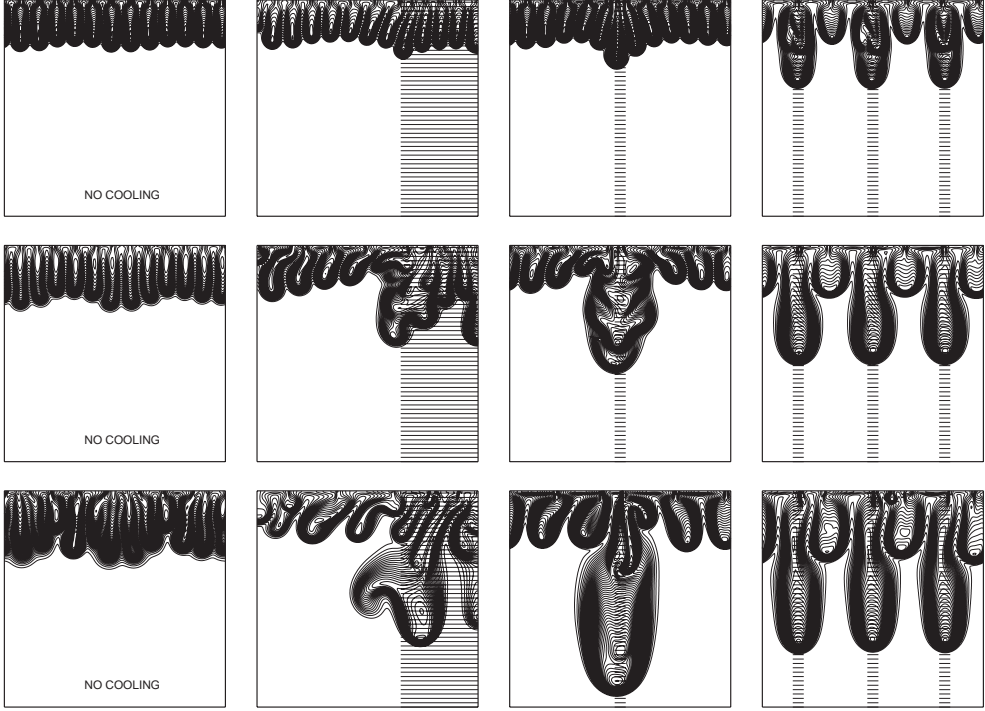


Fig. 2 – Evolution of salt concentration in the lower layer obtained numerically in the cases of no external control (first column) and external localized cooling applied in the dashed zone at a dimensionless time $t^* = 1.8$ (fingering zone, second column), $t^* = 1.8$ (sole finger, third column) and $t^* = 1.0$ (periodic fingering, fourth column). The size of the system is 40×40 . In each column the figures pertain to dimensionless times $t = 2, 2.6, 3.4$ from top to bottom, respectively.

$Bi = 0$ in the outside area kept at room temperature. As initial condition, step functions for concentrations of acid and base coupled with white-noise disturbances for the stream function are used. In order to characterise the nonlinear dynamics, various types of measurements can be done [23]. We focus here on the reaction rate R defined as the area of the reacted zone (*i.e.* the number of points where $S(x, z, t)$ is higher than a threshold S^* which was typically 0.001) normalized by the width of the system [24]:

$$R(t) = \frac{1}{H} \int_{-L}^0 \int_0^H \zeta \, dx \, dz, \quad (12)$$

where $\zeta = 1$ if $S > S^*$ and zero otherwise. Following the temporal evolution of the fingering dynamics and of the reaction rate R allows to show that localized cooling can be used to control the chemo-hydrodynamic pattern and tune the efficiency of the reaction yield. In that respect, the first column in fig. 2 and the solid line in fig. 3 show the evolution in time of the salt concentration and of the reaction rate, respectively, in the absence of any external cooling. The patterns are similar to those observed in the nonperturbed experiments (see fig. 1). As in experiments, the dynamics of the system evolves through two typical stages. First, we observe a pure reaction-diffusion process characterized by the square-root time evolution for the reaction rate (see fig. 3). Then convection arises leading to fingering, which results in a sharp increase of the reaction rate.

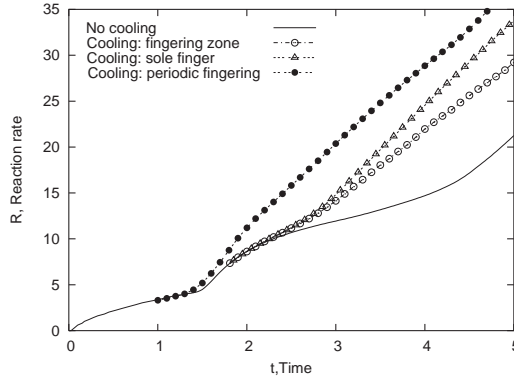


Fig. 3 – Reaction rate R as a function of time for the four simulations of fig. 2.

We found that we can modify this pattern formation and its characteristics, such as reaction rate $R(t)$, by applying an external cooling to the sidewalls of Hele-Shaw cell. The second, third and fourth column in fig. 2 and the corresponding curves in fig. 3 show what happens if a part of the cell (indicated in fig. 2 by the dashed zone) is brought in contact with a highly conductive material at a time t^* after the start of the pattern formation. As in experiment we observe a strengthening of fingering in the cooled area. The immediate growth of the reaction rate following the contact with highly conductive material seen in fig. 3 shows that the chemical reaction adapts without any delay to the flow increase due to the temperature perturbation. In addition to this influence on the yield of reaction, our numerical simulations show that localized cooling not only controls the amount of salt produced but also enhances the mass transfer rate and controls successfully the pattern formation itself. The third and fourth columns of fig. 2 correspond to cases of localized and periodic cooling, respectively. We can see that fingering follows the imposed cooling pattern producing one localized elongated finger in the first case, and a perfect periodic system of fingers in the second case. It should be noted that in both cases the wavelength of the controlled pattern differs from the natural one. Note furthermore that, in our model, $Bi = \infty$ in the cooled area and zero otherwise. Hence, in the numerics, the finger elongation is strictly confined to the cooled area. In the experiment, however, the lateral heat diffusion in the glass plates smears out the temperature distribution imposed, leading to a gradual reduction of the finger length (cf. fig. 1).

The physical mechanism of control is quite simple. By cooling the fluid in a given zone through the sidewall, we extract a part of the reaction enthalpy thereby making the fluid locally heavier than the surrounding fluid. This unstable configuration modifies locally the existing vortex and changes the reaction rate in the way desired by the controller, *e.g.* by the application of an array of cold pieces of metal with a given spacing. It allows for a quick and very flexible control of the whole system.

In summary, we have shown both experimentally and theoretically that chemo-hydrodynamic pattern formation in a Hele-Shaw reactor can be easily and efficiently controlled by using external localized cooling. Such a cooling produces a local convective vortex which influences the dynamics of the system in the way prescribed by the experimentalist. This control depends on i) the geometry, ii) location and iii) temperature of the cooled area as well as iv) the time at which the cooling is switched on and off. By tuning each of these parameters or a combination of them, we obtain a very flexible and easy-to-use technique for control of the pattern. From a technological point of view, the interest lies in the fact that such a control enhances the reaction rate and hence the yield of the reaction as well as the mass transfer across the interface.

* * *

We thank M. ACKER for fruitful discussions and FRFC, SSTC and Prodex (Belgium) as well as DLR and DFG (Germany) for financial support.

REFERENCES

- [1] SHERWOOD T. S. and WEI J. C., *Ind. Eng. Chem.*, **49** (1957) 1030.
- [2] AVNIR D. and KAGAN M., *Nature*, **307** (1984) 717.
- [3] MICHEAU J.-C., GIMENEZ M., BORCKMANS P. and DEWEL G., *Nature*, **305** (1983) 43.
- [4] ECKERT K. and GRAHN A., *Phys. Rev. Lett.*, **82** (1999) 4436.
- [5] ECKERT K., ACKER M. and SHI Y., *Phys. Fluids*, **16** (2004) 385.
- [6] ERMAKOV S. A., ERMAKOV A. A., CHUPAKHIN O. N. and VAISSOV D. V., *Chem. Eng. J.*, **84** (2001) 321.
- [7] KARLOV S. P., KAZENIN D. A. and VYAZMIN A. V., *Physica A*, **315** (2002) 236.
- [8] IBANEZ J. L. and VELARDE M. G., *J. Phys. Lett.*, **38** (1977) 1479.
- [9] CITRI O., KAGAN M. L., KOSLOFF R. and AVNIR D., *Langmuir*, **6** (1990) 559.
- [10] SIMANOVSKII I. B. and NEPOMNYASHCHY A. A., *Convective Instabilities in Systems with Interface* (Gordon and Breach, New York) 1993.
- [11] BRATSUN D. A. and DE WIT A., *Phys. Fluids*, **16** (2004) 1082.
- [12] LIN A. L. *et al.*, *Phys. Rev. Lett.*, **84** (2000) 4240.
- [13] HILDEBRAND M., SKØDT H. and SHOWALTER K., *Phys. Rev. Lett.*, **87** (2001) 088303.
- [14] STEINBOCK O., ZYKOV V. and MÜLLER S. C., *Nature*, **366** (1993) 322.
- [15] PETROV V., OUYANG Q. and SWINNEY H. L., *Nature*, **388** (1997) 655.
- [16] SCHMIDT B., DE KEPPER P. and MÜLLER S. C., *Phys. Rev. Lett.*, **90** (2003) 118302.
- [17] HORVÁTH A. K. *et al.*, *Phys. Rev. Lett.*, **83** (1999) 2950.
- [18] RÜDIGER S. *et al.*, *Phys. Rev. Lett.*, **90** (2003) 128301.
- [19] BURGESS J. M. *et al.*, *Phys. Rev. Lett.*, **86** (2001) 1203.
- [20] HOWLE L. E., *Int. J. Heat Mass Transfer*, **40** (1997) 822.
- [21] GARNIER N., GROGORIEV R. O. and SCHATZ M. F., *Phys. Rev. Lett.*, **91** (2003) 054501.
- [22] ROGERS J. L., SCHATZ M. F., BRAUSCH O. and PESCH W., *Phys. Rev. Lett.*, **85** (2000) 4281.
- [23] DE WIT A., *Phys. Fluids*, **16** (2004) 163.
- [24] CONSTANTIN P., KISELEV A., OBERMAN A. and RYZHIK L., *Arch. Ration. Mech. Anal.*, **154** (2000) 53.